HHS Public Access

Author manuscript

J Comp Neurol. Author manuscript; available in PMC 2017 February 01.

Published in final edited form as:

J Comp Neurol. 2016 February 1; 524(2): 309–322. doi:10.1002/cne.23844.

Synaptic ultrastructure changes in trigeminocervical complex post trigeminal nerve injury

John Park[1], **Van Nancy Trinh**[2], **Ilse Sears-Kraxberger**[3], **Kang-Wu Li**[2], **Oswald Steward**[3], and **Z. David Luo**[1,2,3]

[1]Department of Pharmacology, University of California Irvine, School of Medicine, Irvine, CA 92697

[2]Department of Anesthesiology & Perioperative Care, University of California Irvine, School of Medicine, Irvine, CA 92697

[3]Reeve-Irvine Research Center, University of California Irvine, School of Medicine, Irvine, CA 92697

Abstract

Trigeminal nerves collecting sensory information from the orofacial area synapse on second order neurons in the dorsal horn of subnucleus caudalis and cervical C1/C2 spinal cord (Vc/C2, or trigeminocervical complex), which is critical for sensory information processing. Injury to the trigeminal nerves may cause maladaptive changes in synaptic connectivity that plays an important role in chronic pain development. Here, we examined whether injury to the infraorbital nerve, a branch of the trigeminal nerves, led to synaptic ultrastructural changes when the injured animals have developed neuropathic pain states. Transmission electron microscopy was used to examine synaptic profiles in Vc/C2 at three-weeks post-injury, corresponding to the time of peak behavioral hypersensitivity following chronic constriction injury to the infraorbital nerve (CCI-ION). Using established criteria, synaptic profiles were classified as associated with excitatory (R-), inhibitory (F-), and primary afferent (C-) terminals. Each type was counted within the superficial dorsal horn of the Vc/C2 and the means from each rat were compared between sham and injured animals; synaptic contact length was also measured. The overall analysis indicates that rats with orofacial pain states had increased numbers and decreased mean synaptic length of R-profiles within the Vc/C2 superficial dorsal horn (lamina I) three-weeks post CCI-ION. Increases

Corresponding author: Dr. Z. David Luo, Department of Anesthesiology & Perioperative Care, University of California Irvine, Gillespie Bldg, Rm 3113, 837 Health Sci. Rd., Irvine, CA 92697.

Conflict of Interest

O.S. is one of the cofounders of a company called “Axonis,” which holds options on patents relating to PTEN deletion and axon regeneration. Other authors declare no conflicts of interest.

Resources Cited

Model Organisms: Experiments were conducted in rattus norvegicus strain SD (RRID:RGD_70508)

Tools, Software, and Database: Image analysis was conducted with Image J software (http://rsb.info.nih.gov/ij, RRID:nif-0000-30467) and Graphpad Prism (www.graphpad.com, RRID:rid_000081)

Role of authors

All authors had full access to all the data in the study and take responsibility for the integrity of the data and the accuracy of the data analysis. Study concept and design: JP, OS, ZDL. Acquisition of data: JP, VNT, ISK, KWL. Analysis and interpretation of data: JP, VNT, OS, ZDL. Drafting of Manuscript: JP, ZDL. Critical revision of the manuscript for important intellectual content: JP, OS, ZDL. Statistical analysis: JP. Obtained funding: OS, ZDL. Administrative, technical, and material support: JP, VNT, ISK, KWL, OS, ZDL. Study supervision: ZDL.

in the number of excitatory synapses in the superficial dorsal horn of Vc/C2 could lead to enhanced activation of nociceptive pathways, contributing to the development of orofacial pain states.

Keywords

synaptic ultrastructure; trigeminal nerve injury; orofacial neuropathic pain

Introduction

Trigeminal nerve injuries can lead to the development of neuropathic pain, which is debilitating and difficult to treat (Bennetto et al., 2007; Zakrzewska and McMillan, 2011). This disorder can lead to pain sensations with innocuous stimuli (allodynia) or exaggerated pain sensations with supra-threshold stimuli (hyperalgesia) (Iwata et al., 2011; Zakrzewska and McMillan, 2011). Mechanisms underlying neuropathic pain are not well understood. Recently, our group and others have reported that neuropathic pain can be attributed, at least in part, to synaptic changes in the neuronal circuitry of the spinal cord that may mediate injury-induced pain sensations (Sandkuhler, 2009; Li et al., 2014a; Li et al., 2014b).

The trigeminocervical complex, including spinal subnucleus caudalis and cervical C1/C2 spinal cord (Vc/C2), is the major projection site for trigeminal nerves transmitting both noxious and non-noxious information (Sessle, 2000). The Vc/C2 receives nociceptive information through glutamatergic peripheral inputs (Hu, 1990; Bae et al., 2000). Vc/C2 neuron excitability is significantly enhanced after trigeminal nerve injury due to increased receptive field sizes, basal level and evoked hyperexcitability that reflect central sensitization (Iwata et al., 2001; Iwata et al., 2004; Tsuboi et al., 2004; Chiang et al., 2005; Li et al., 2014b). Also, local inhibitory γ-aminobutyric acid (GABAergic) and/or glycinergic interneurons have been shown to modulate Vc/C2 neuron activities (Jacquin et al., 1989; Avendano et al., 2005; Bae et al., 2005) and pre-synaptic inhibition of primary afferent terminals (Todd, 1996). There is evidence for reduced inhibitory transmission in the superficial spinal dorsal horn and spinal trigeminal nucleus (Moore et al., 2002; Martin et al., 2010) that may be due to loss in GABA-immunoreactive neurons (Castro-Lopes et al., 1993; Ibuki et al., 1997; Eaton et al., 1998; Moore et al., 2002; Somers and Clemente, 2002; Martin et al., 2010). Thus, alterations in excitatory or inhibitory synapses or both may contribute to chronic orofacial pain states, and alterations could involve changes in synaptic function or in the number or size of existing synapses.

The goal of the present study was to assess whether there were detectable changes in excitatory or inhibitory synapses in the afferent recipient zone of the trigeminocervical complex in a rat model of chronic constriction injury of the infraorbital nerve (CCI-ION), which leads to orofacial neuropathic pain. The ION branch of the trigeminal nerve is exclusively sensory and nociceptive fibers that project to different laminae in the dorsal horn of Vc/C2 (Morris et al., 2004; Todd, 2010). We focused our analysis within the superficial dorsal horn (laminae I-II) because these layers are known to receive major nociceptive

inputs; and at three-weeks after CCI-ION injury because this is when the injured animals have peak orofacial hypersensitivity (Vos et al., 1994; Li et al., 2014a).

Materials and Methods

Experimental Animals

Six adult male Harlan Sprague-Dawley rats weighing approximately 200g were used for this study (RRID:RGD_70508). The animals were exposed to 12 h light/12 h dark cycle with food and water available *ad libitum*. The animal usage and experimental protocols were approved by Institutional Animal Care and Use Committee of the University of California Irvine.

Surgery

The unilateral chronic constriction injury to the infraorbital nerve (ION) was performed as described (Kernisant et al., 2008). Briefly, isoflurane anesthetized rats with hair shaved above the left eye were put in a stereotaxic frame. An anterior-posterior skin incision was made above the left eye following the curve of the frontal bone. The ION lying on the maxillary bone was exposed and dissected free from surrounding connective tissue within the orbit. Fine forceps and a silk suture (5–0) loaded needle with a bent tip were used to place two loose ligations around the ION, 3–4 mm apart. Sham operated animals were similarly prepared with no ION ligation. The skin incision above the eye was sutured with silk sutures (5–0) and rats were placed on a warm heating pad until they recovered from the anesthetic.

Behavioral Testing

Orofacial behavioral testing was performed in a blinded fashion as described (Vos et al., 1994; Li et al., 2014a). Briefly, the vibrissal pad was shaved under light isoflurane anesthesia one day before the behavioral test. Rats were habituated at least one hr prior to behavioral testing. Orofacial mechanical sensitivity to von Frey filament stimulation was assessed with a series of von Frey filaments (numbers 3.61, 3.84, 4.08, 4.31, 4.56, 4.74, 4.93 and 5.18; equivalent to 0.4, 0.6, 1.0, 2.0, 4.0, 6.0, 8.0 and 153g of force, respectively) with Dixon's Up-Down method (Dixon, 1980) on both sides of the vibrissal pad. The following behaviors were considered a positive response to von Frey filaments: 1) a brisk withdrawal reaction; 2) an escape/attack reaction in which a rat avoided the filament either by moving away from the filament to assume a crouching position against a cage wall or burying its head under the body after stimulation, or attacked the filament by biting and grabbing; 3) asymmetric face grooming shown as at least three uninterrupted face-wash strokes directed to the facial area being stimulated, often preceded by a brisk withdrawal reaction. Presence or absence of a positive response prompted the use of the next lower or higher stimulating force, respectively, which was repeated for a total of six responses to von Frey stimuli. The 50% withdrawal threshold values were calculated using the formula: $10^{(X+kd)}/10^4$, where X is the value of the final von Frey filament used in log units, k is the tabular value for the positive/negative response patterns from Chaplan et al. (Chaplan et al., 1994) and d is the mean differences between stimuli in log units. Scores of 0.25 or 153g were assigned, respectively, when consecutive positive or negative responses were observed.

Electron Microscopy

CCI-ION and sham rats were perfused with 2% paraformaldehyde/2% glutaraldehyde (pH 7.4) three-weeks post CCI-ION, which correlates with orofacial hypersensitivity in the injury side of CCI-ION rats (Li et al., 2014). The Vc/C2 was isolated, rinsed in 0.1M sodium cacodylate buffer (pH 7.4), and post-fixed in 1% osmium tetroxide in 0.1M sodium cacodylate buffer for 1 hour, dehydrated in increasing serial dilutions of ethanol (70%, 85%, 95%, 100%) for 10 min each, incubated in propylene oxide for 1 hour, incubated in propylene oxide/Spurr's resin (1:1) for 1 hour, and then embedded in Spurr's resin overnight. Ultrathin sections (~60nm thickness) were cut by a researcher blinded to the surgery procedures and behavioral outcomes using a *Leica* Ultracut UCT ultramicrotome (*Leica*, Vienna, Austria), mounted on copper grids, stained with uranyl acetate and lead citrate. Images of the Vc/C2 were viewed on a JEOL 1400 transmission electron microscope (JEOL, Tokyo, Japan) and images were captured using a Gatan Digital camera (Gatan, Pleasanton, CA, USA).

Image Processing

The sampling procedure was performed as described by Darian-Smith et al. (Darian-Smith et al., 2010). Briefly, synapses in electron micrographs (5000X) were counted along 12 tracks (approximately 15μm each) taken at different depths and running orthogonal to the curve of the dorsal horn, starting from the dorsal border of the dorsal horn grey matter and covering approximate 180μm in depth as outlined in Figure 2 (A and B). Data from tracks were combined based on reported approximate dorso-ventral lamina thicknesses as the following: 0 to 30μm (lamina I), 30 to 135μm (lamina II), and 135 to 180μm (border region of lamina II inner and III, or lamina IIi/III) (Gobel, 1978; Alvarez and Priestley, 1990; Chery et al., 2000; Yasaka et al., 2010). The thickness of lamina I in rat cervical dorsal spinal cord arrange from 15–50μm depending on sample orientation and sectioning (Chery et al., 2000), so we used 30μm for lamina I in our study. Since the transition zones between laminae are difficult to define in the rat (Todd et al., 1998; Chery et al., 2000), this lamina division approach is an estimate only. In each non-overlapping image, the following synapse types were identified: **R** = synapses with round vesicles, asymmetric synapse, and a single large synaptic contact (presumed to be excitatory); **C** = large presynaptic terminal with round vesicles and often form multiple synaptic contacts and contain dense-cored vesicles (presumed to be primary afferent axons); **F** = presynaptic terminals with pleomorphic-flattened vesicles and symmetric synapses (presumed to be inhibitory synapses). An observer who was blinded for animal groups identified these synaptic profiles from each image.

To identify changes in the proportion of a particular type of synaptic profile after CCI-ION, counts of each synaptic profile were divided by the total of all synaptic profile counts across all tracks per dorsal horn section and expressed as a percentage of total synaptic counts. Synaptic profile numbers for each track were also normalized to area of $100\mu m^2$. To determine whether any changes in synaptic profile numbers were actual changes in particular synapse types, but not changes in size of the profiles, we estimated their numerical density by using the size-frequency method (DeFelipe et al., 1999). The number of synapse profile per unit volume was estimated using the formula $N_v = N_A/d$, in which "N_A" is the

number of a particular type of synapses per unit area and "d" is the average length of corresponding synaptic densities (μm). The synapse length provides a normalization factor for sampling bias introduced by tissue thickness. For all synapses identified, the post-synaptic density length was measured using ImageJ software (RRID:nif-0000-30467).

To determine if unilateral CCI-ION injury caused bilateral effects on synaptic profiles, sham rats were also included as controls for comparisons using univariate analysis of variance (ANOVA). For changes in total synaptic profile counts, one-way ANOVA with *post hoc* Bonferroni tests was used to compare data between the ipsilateral and contralateral Vc/C2 of both CCI-ION and sham rats. For laminar specificity, data from the ipsilateral and contralateral Vc/C2 of CCI-ION rats were compared with that from the ipsilateral and contralateral Vc/C2 of sham rats using a mixed two-way ANOVA analysis, followed by Bonferroni or Fisher's LSD *post hoc* test between tracks (ipsilateral vs. contralateral Vc/C2 of CCI-ION; or ipsilateral/contralateral Vc/C2 of sham). Non-parametric one-way ANOVA with Dunn's multiple comparison *post hoc* test was also used as an alternative statistical analysis as indicated. All statistical analysis were performed by using PRISM 6.0 (RRID:rid_000081, Graphpad, San Diego, CA).

Results

We examined whether there were changes in the number of different types of synapses during the development of chronic orofacial pain after CCI-ION. As shown in Figure 1, unilateral CCI-ION injury caused a reduction in orofacial threshold to von Frey filament stimuli, or tactile allodynia, on the injury side three weeks post-surgery compared with that from the non-injury side and sham operated rats. This is consistent with previous reports from this model (Vos et al., 1994; Li et al., 2014a). Thin sections of the Vc/C2 spinal cord were collected from CCI-ION and sham rats three weeks post-surgery and examined for synaptic changes. Profiles were identified and counted from 12 most superficial tracks (approximately 15μm each) running orthogonal to the curve of the dorsal border of dorsal spinal cord grey matter and covering superficial dorsal horn as shown in Figure 2A and B. We combined data from tracks that correspond to the predicted thickness of laminae I (top 2 tracks, 0–30μm) (Chery et al., 2000), II (7 tracks, 30–135μm) (Yasaka et al., 2010), and border region of II inner and III (IIi/III) (3 tracks, 135–180μm) for analysis in an attempt to identify any laminar specificity. Figure 2C–E shows typical examples of each type of profile quantified in our analysis. The R-profiles were defined as having a single asymmetric synapse (large post-synaptic density) with round vesicles (Figure 2C). In contrast, C-profiles were large, contain round and dense core vesicles, and often form multiple asymmetric synapses (Figure 2E). The F-profiles contained pleomorphic vesicles and form symmetrical synapses (Figure 2D).

Table 1 shows the total number of each synaptic profile (R-, F-, and C-profile) counted and the total area of Vc/C2 dorsal horn analyzed across all tracks. A total of 4,516 and 5,041 profiles were quantified from three CCI-ION and sham-operated animals, respectively. Each profile type was normalized with respect to the tissue area examined (per 100μm^2) or expressed as a proportion of total profiles summed across all tracks per animal. Profile counts for R synapses were similar across groups. Counts for F synapses were higher

ipsilateral to the CCI-ION injury than in the other groups, but differences were not statistically significant. Counts for C synapses were very similar on the two sides of CCI-ION rats, and these values were lower than either sham group, but again these differences were not statistically significant (Table 1; Figure 3A and B). It is important to note that the lack of a significant difference cannot be taken as indicating no effect because of the low "n". Since the total areas of Vc/C2 dorsal horn sections examined were not significantly different between CCI-ION and sham rats (Figure 3C), potential sampling bias of synaptic profile counts is less likely.

Table 2 shows over all data interactions among experimental groups and/or laminae based on the primary statistical analysis with two-way ANOVA. Statistically significant changes were indicated in R-synaptic profile numbers and length when comparing data from all experimental groups and laminae (top, see specific changes below). As for lamina-specific interactions, statistically significant changes were indicated for the number, but not the length, of all synaptic profiles (R-, F-, and C-) (bottom). However, there was no significant injury-induced difference (effect) on total R-, F-, or C-synaptic profiles counts in superficial dorsal horn among experimental groups (middle), which is in agreement with the results shown in Table 1 and Figure 3.

CCI-ION injury led to increased R-profiles in superficial dorsal horn

Per Unit Area—To examine the laminar specific difference in the synaptic profile numbers after CCI-ION, we quantified each synapse profile type per 100μm^2 at the superficial laminae of the dorsal horn, and compared data (mean of each animal) from the ipsilateral CCI-ION to that from contralateral CCI-ION and ipsilateral/contralateral sham using two-way ANOVA with Bonferroni *post hoc* test (Figure 4). In general, there are more R- and C-profiles in the more superficial laminae (Figure 4A and C) but more F-profiles in the deeper laminae (Figure 4B), which is consistent with the general anatomical distribution of excitatory, nociceptive and inhibitory neurons in the dorsal horn (Todd, 2010; Braz et al., 2014). Two-way ANOVA revealed a significant group effect for the R-, but not the F- and C-profile synapse counts per 100μm^2 (R-Profiles [$F(6,16)=3.02$; $p=0.04$], F-profiles [$F(6,16)=1.85$; $p=0.15$], and C-Profiles [$F(6,16)=0.52$; $p=0.79$], see Table 2). Follow-up assessments of group differences in R-synapse profile counts by Bonferroni's multiple comparisons test revealed that R-synapse counts were significantly higher in the CCI-ION-Ip group (2.66±0.46 per 100μm^2) compared with CCI-ION-C (1.14±0.01) ($p=0.0009$) and Sham-Ip (1.52±0.12) ($p=0.0167$); the value for the Sham-C group (1.80±0.34) is not significantly different from CCI-ION-Ip ($p=0.1333$) in lamina I (Figure 4A).

Although the two-way ANOVA did not reveal a significant Groups effect for F-synapses, there was a trend that F-synapse counts in lamina II of the injury side (CCI-ION-Ip) were higher than other groups (Figure 4B). We were concerned about the possibility of a Type II statistical error because of low "n". Strictly speaking, follow-up multiple comparisons are not justified unless there is an overall group effect in the two-way ANOVA, but we did feel that it was important to further test for potential differences in F-synapse counts in lamina II (CCI-ION-Ip, 5.10±1.04; CCI-ION-C, 3.65±0.83; Sham-Ip, 3.92±0.43; Sham-C, 3.60±0.05). There were no differences between groups using Bonferroni-adjusted correction (CCI-ION-

Ip vs. CCI-ION-C, p=0.69; CCI-ION-Ip vs. Sham-Ip, p=0.27). However, uncorrected Fisher's LSD test revealed that differences between CCI-ION-Ip and Sham-Ip were statistically significant (p=0.03), but differences between CCI-ION-Ip and CCI-ION-C were not statistically significant (p=0.08). The uncorrected Fisher's LSD test is not rigorous here because of the multiple comparisons, but taken together, the analyses indicate that a possible increase in F-synapses in layer II cannot be excluded.

Because of concerns for the possibility of a type II statistical error, especially in terms of F-profiles, we also carried out an alternative statistical analysis using non-parametric Kruskal-Wallis test. The main conclusions based on Kruskal-Wallis were similar; R-profiles were significantly higher in superficial laminae on the side of the injury (CCI-ION-Ip p=0.004). There was a trend for a difference in F-profiles that was not statistically significant (p=0.11), and there was no significant difference in C-Profiles (p=0.79).

Volumetric Density—To ensure that changes in profile types observed in Figure 4 were not due to sampling bias, we used the size-frequency method (DeFelipe et al., 1999; Darian-Smith et al., 2010) to estimate the mean value of profiles per unit volume in each animal and compared data from the CCI-ION ipsilateral dorsal horn with that from the CCI-ION contralateral and sham ipsilateral/contralateral dorsal horn using two-way ANOVA with Bonferroni *post hoc* test (Figure 5). Two-way ANOVA analysis of the synaptic profile counts per $100\mu m^3$ in Table 2 revealed a significant group difference for R-Profiles, [F(6,16)=4.12, p=0.01], but not for F-profiles [F(6,16)=1.98, p=0.13] or C-Profiles [F(6,16)=1.04, p=0.44]. Follow-up assessments of group differences in R-synapse profile counts by Bonferroni's multiple comparisons test revealed that R-synapse counts were significantly higher in the CCI-ION-Ip group (11.49±2.27) compared to the CCI-ION-C (4.03±0.07) (p=0.0003), Sham-Ip (5.28±0.34) (p=0.0023), and Sham-C group (6.92±1.37) (p=0.0383) in lamina I (Figure 5A).

As above, out of concern for a type II error, we carried out follow-up assessments of F-profile counts in lamina II although the two-way ANOVA did not reveal a significant group effect. The same patterns of results were seen as above. There were no statistically significant differences between groups using Bonferroni-adjusted correction (CCI-ION-Ip vs. CCI-ION-C, p=0.68; CCI-ION-Ip vs. Sham-Ip, p=0.34). However, uncorrected Fisher's LSD test revealed that differences between CCI-ION-Ip and Sham-Ip (p=0.04) or Sham-C (p=0.04) were statistically significant, but differences between CCI-ION-Ip and CCI-ION-C were not statistically significant (p=0.08) in lamina II (Figure 5B).

The alternative analysis of the volume density data by non-parametric Kruskal-Wallis test yielded the same main conclusions as the two-way ANOVA. R-profiles were significantly higher in superficial laminae on the side of the injury (CCI-ION-Ip p=0.004). There was a trend for a difference in F-profiles that was not statistically significant (p=0.19), and there was no significant difference in C-Profiles (p=0.51).

Synapse Length—To evaluate the strength of synaptic contacts associated with different synaptic profile types, we measured the post-synaptic length for each profile type, a parameter that is associated with changes in synaptic efficacy and plasticity (Desmond and

Levy, 1986; Pierce and Lewin, 1994). Two-way ANOVA revealed a significant group difference for R-Profiles [F(6,16)=4.61, p=0.007], but not for F-profiles [F(6,16)=1.01, p=0.45] and C-Profiles [F(6,16)=2.06, p=0.12] (Table 2). Follow-up assessments of group differences by Bonferroni's multiple comparisons test revealed that mean post-synaptic length of R-synapses was significantly shorter in the CCI-ION-Ip group (0.23±0.007μm) compared with Sham-Ip (0.29±0.02μm) (p=0.035) in lamina I. The value for the CCI-ION-Ip group in lamina I was not significantly different from that of the CCI-ION-C (0.28±0.006μm) (p=0.709) and Sham-C (0.26±0.007μm) (p=0.974), respectively (Figure 6A). Also, values for post-synaptic length of F- and C-synaptic profiles in different laminae were not significantly different (Figure 6B, C).

The alternative analysis of the data on synapse length by the Kruskal-Wallis test confirmed the group differences in synaptic length for R-profiles (p=0.02). In addition, the Kruskal-Wallis test indicated significant group differences for the F-Profiles in lamina II (p=0.002) and C-Profiles in lamina I (p=0.02). Dunn's multiple comparison post-hoc test indicated that average post-synaptic length of F-synapses was significantly shorter in the CCI-ION-Ip group compared with that in the Sham-C group (p=0.007) in lamina II, and average length of C-synapses in the CCI-ION-Ip group was significantly shorter than that in the Sham-Ip group (p=0.04) in lamina I.

Length distributions—We were curious whether the differences in mean length were due to changes in the number of short or long postsynaptic lengths vs. a shift in the distribution. To address this question, we assessed the length distributions by binning values into size categories and illustrated these by histograms (Figure 7). There were more R- and C-profiles in the shortest length category in the CCI-ION-Ip group, but these differences alone were not of sufficient magnitude to account for the differences in the means. This suggests that the changes in the mean were a result of a shift in the distribution rather than the appearance of synapses with particular long or particularly short postsynaptic lengths.

Discussion

Our previous studies have indicated that CCI-ION trigeminal nerve injury leads to aberrant excitatory synaptogenesis in the superficial dorsal horn of trigeminocervical complex (Vc/C2) that correlates with dorsal horn neuron sensitization and orofacial neuropathic pain states (Li et al., 2014b). This suggests that nerve injury-induced aberrant synaptogenesis is likely a form of neuroplasticity underlying the development of orofacial neuropathic pain post trigeminal nerve injury. However, it is not clear if this nerve injury-induced maladaptive change affects the number and/or strength of different synapse types. In the present study, we examined synapse ultrastructure in superficial dorsal horn of Vc/C2 from sham and CCI-ION rats three-weeks post injury when the injured rats exhibit severe orofacial pain states (Figure 1) (Li et al., 2014a). Our data indicate that trigeminal nerve injury leads to an increase in R-synaptic profiles (presumably excitatory synapses) and a decrease in R-synaptic length in lamina I of Vc/C2. There was a trend for increased F-synapses in lamina II that were not statistically significant by two-way ANOVA with multigroup comparisons, but that did reach statistical significance with uncorrected Fisher's LSD test. Also, the Kruskal-Wallis test revealed significant decreases in F- and C-synaptic

length in lamina II and I, respectively, suggesting an overall decrease in synaptic lengths post CCI-ION injury. Overall, our data support that CCI-ION leads to changes in excitatory synapses in lamina I. The nature of the changes is consistent with increased excitatory synaptic input to second order nociceptive neurons that could explain the development of orofacial neuropathic pain states. Our data do not exclude the possibility of changes in inhibitory synapses in lamina II, but how these changes could contribute to neuropathic pain is less evident.

Changes in number and size of R synapses

To ensure that the increase in R-synaptic profiles was not due to an increase in size of R-profiles that could increase the likelihood of detecting the same profile more than once in individual micrographs, we applied the size-frequency method to correct for sampling biases introduced by the fact that the synapses are several times larger than the tissue section thickness. This sampling method has been shown to be efficient in analyzing large areas in spinal dorsal horn and reducing variations across samples (DeFelipe et al., 1999; Benes and Lange, 2001; Darian-Smith et al., 2010). Our data indicate that findings from the size-frequency method correlate well with results of synaptic profile counts per unit area, confirming an increase in the number of R-profiles, presumably excitatory synapses, in superficial dorsal horn of the injury side three-weeks after CCI-ION injury compared to that from non-injury side of CCI-ION and sham control rats.

A potential limitation in this synapse-profiling scheme is that an identified “R-profile” could be a “C-Profile” since both profiles share similar structural morphology, except that dense core vesicles are associated with C-profile primary afferent fibers (Ribeiro-da-Silva et al., 1989; Bailey and Ribeiro-da-Silva, 2006), which could be lost during thin section preparation. However, this is unlikely the case due to the excellent fixation, and preservation of tissue integrity in our study (Fig. 2). In addition, our conclusion is supported by our previous data indicating that almost all CCI-ION-induced synapses in superficial dorsal horn of Vc/C2 contain VGLUT2 vesicular glutamate transporter (Li et al., 2014b), which is expressed in many of the excitatory interneurons (Oliveira et al., 2003; Todd et al., 2003; Maxwell et al., 2007; Santos et al., 2009; Yasaka et al., 2010; Braz et al., 2014), and myelinated, but not unmyelinated (C-type), afferents in lamina I (Todd et al., 2003). This suggests that increased excitatory synapses in superficial dorsal horn post nerve injury may have direct effects on at least orofacial tactile allodynia (Li et al., 2014b), which is transmitted mainly by myelinated sensory fibers (Julius and Basbaum, 2001). Interestingly, genetic ablation of VGLUT2, but not VGLUT1, attenuates nerve-injury induced tactile allodynia, cold and thermal hyperalgesia (Leo et al., 2009; Rogoz et al., 2012). Since cold and thermal hyperalgesia are mainly transmitted by unmyelinated nociceptive afferents (Julius and Basbaum, 2001), it is possible that increased synapses on excitatory interneurons contribute to hypersensitivities to these modalities indirectly. Further functional studies are warranted to further delineate the functionality of nerve injury-induced R-synaptic profiles.

A significant decrease in mean synaptic length of R-profiles was also observed within lamina I of Vc/C2 superficial dorsal horn from the injury side of CCI-ION rats compared with that from non-injury side of CCI-ION and sham rats. Synaptic length, the length of

post-synaptic density along the parallel pre- and post-synaptic membranes of the profiles, is a structural correlate of synaptic strength (Pierce and Lewin, 1994). Thus, taken in isolation, the decrease in average synapse length would predict decreases in average excitatory synaptic strength. On the other side, however, the decrease in average R-profile synaptic length is associated with an increase in the number of R-synaptic profiles within lamina I. One possibility is a selective formation of new R-type excitatory synapses with shorter synapse lengths after nerve-injury. However, histograms of length distributions do not support this interpretation since there is no evidence of a selective increase in synapses with short postsynaptic lengths that would account for the shift in the mean.

Our data also indicate a decrease in average synaptic lengths of C-profiles in lamina I. This difference was not significant by ANOVA but did reach statistical significance with the non-parametric Kruskal-Wallis test. Thus, we could not exclude completely if peripheral nerve injury may affect C-type synapse sizes.

Since lamina I is the major site for relaying nociceptive information from primary afferent fibers, increased excitatory synaptic connections to interneurons and/or projection neurons within lamina I could facilitate the activation of projection neurons, thereby contributing to behavioral hypersensitivity after nerve-injury. However, the detailed synaptic connectivity of these changes in lamina I remains unclear. Studies have shown that excitatory interneurons within lamina II can integrate inputs from primary afferents and interneurons locally, and provide excitatory synaptic inputs to lamina I projection neurons (Lu and Perl, 2005; Yasaka et al., 2007; Kato et al., 2009; Todd, 2010; Braz et al., 2014). Excitatory interneuron activation by primary afferent fibers is considered an additional feed-forward excitatory pathway, which together with direct activation of lamina I projection neurons by nociceptive fibers, contributes to chronic pain states (Braz et al., 2014). Further studies are needed to understand how the increases in excitatory synapses that we show here actually alter circuit function in dorsal horn excitatory circuitry after nerve-injury.

Alterations in inhibitory circuitry?

The contributory role of inhibitory interneurons to neuropathic pain states remains controversial due to conflicting findings from neuropathic pain models. Some studies have reported a reduction of GABAergic inhibitory transmission in lamina II neurons following chronic constriction injury (CCI) or spared nerve injury (SNI) of the sciatic nerve (Moore et al., 2002) and a substantial loss of GABA-immunoreactive neurons following CCI (Ibuki et al., 1997; Eaton et al., 1998; Martin et al., 2010). These changes could lead to the loss of inhibitory input onto excitatory neurons, or disinhibition, in spinal superficial dorsal horn, which could contribute to chronic pain states after nerve injury (Castro-Lopes et al., 1993; Ibuki et al., 1997; Eaton et al., 1998; Moore et al., 2002; Somers and Clemente, 2002). Other stereological studies have reported no loss of inhibitory neurons, or change in GABA-immunoreactivity in the superficial dorsal horn following CCI (Polgar et al., 2003; Polgar et al., 2004) even though the animals develop behavioral hypersensitivity. In the present study, there was no decrease in the number of F-synaptic profiles, as would be predicted if there was a loss of inhibitory neurons or synapses; indeed, in both the counts per area and counts per volume, numbers of F-synapses were slightly higher in lamina II although the

differences were not statistically significant. If there are actually increases in the number of F-synapses, this could lead to increased inhibitory input to inhibitory interneurons leading to dis-inhibition and enhanced net excitatory activity in pain circuits.

Although our data suggest that the major change in CCI-ION injury-induced neuropathic pain states involves excitatory synapses, we cannot rule out the possibility of contribution from localized synaptic changes, or other inhibitory mechanisms such as changes in expression of inhibitory receptors, and synthesis and release of inhibitory neurotransmitters. It is noteworthy that F-synapse length was the shortest in the CCI-ION Ip group in lamina II. Differences were not statistically significant by ANOVA, but the number of animals was small, and the statistical tests were conservative because of Bonferroni corrections. With the non-parametric Kruskal-Wallis test, differences in F-synapse length were significant, however, and decreased synapse length could indicate a decrease in inhibitory synaptic transmission.

Are synaptic changes restricted to the ipsilateral side?

Bilateral behavioral hypersensitivity has been reported in the CCI-ION model although hypersensitivity on the contralateral side is much less severe (Vos et al., 1994; Martin et al., 2010; Li et al., 2014a). Mechanisms responsible for a change in sensitivity on the side contralateral to the CCI are unknown. One possibility is that trigeminal primary afferents project to the contralateral Vc/C2 region (Hockfield and Gobel, 1982), so it is possible that CCI also induces synaptic changes on the contralateral side. The increases in R-synapses we describe here are specific to the side of the injury, and our data reveal no hint of similar synaptic changes on the contralateral side. Indeed, numbers of R-synapses are actually lower on the contralateral side than in the sham controls. Other possible explanations for bilateral hypersensitivity are systemic effects such as bilateral activation of microglial cells and over production of cytokines post injury (Anderson and Rao, 2001; Milligan et al., 2003; Huang and Yu, 2010). These bilateral effects post CCI-ION injury are not specifically correlated with the onset and duration of orofacial pain states (Vos et al., 1994; Martin et al., 2010; Li et al., 2014a). The detectable alterations in R-synapses in the recipient layers that we document here do occur in conjunction with the onset of orofacial pain and occur selectively on the ipsilateral side, where orofacial hypersensitivity is maximal. These features strengthen the conclusion that increases in R-synapses at least partially contribute to the development of orofacial hypersensitivity.

Possible changes in circuit function

Spinal neurons are heterogeneous and include, but are not limited to, projection neurons, excitatory and inhibitory interneurons. Sensory afferents projecting to Vc/C2 dorsal horn can form direct synaptic connections with these neurons, and excitatory or inhibitory interneurons can directly or indirectly modulate the activity of projection neurons, and/or other interneurons through specific synaptic connections (Braz et al., 2014). This well-organized spinal circuitry, in conjunction with descending modulation, forms the structural basis for sensory information processing at the level of trigeminocervical complex. In order to understand the role of nerve injury-induced aberrant synaptic neurotransmission in orofacial pain processing, it is critical to understand the nature of injury-induced changes in

synaptic ultrastructure. Our findings presented here indicate that increased excitatory synapses in lamina I within the superficial dorsal horn correlate with severe orofacial neuropathic pain states after trigeminal nerve injury, supporting a role of this injury-induced plasticity in mediating neuropathic pain states. This is consistent with our recent findings that CCI-ION injury leads to concurrent induction in the Vc/C2 regions of two important synaptogenic proteins, the calcium channel alpha-2-delta-1 subunit (Li et al., 2014b) and thrombospondin-4 (Li et al., 2014a). Interaction of these proteins can promote excitatory synaptogenesis (Eroglu et al., 2009). In conclusion, our findings support that trigeminal nerve injury leads to maladaptive excitatory synaptic plasticity that likely contributes to central sensitization and orofacial neuropathic pain states (Li et al., 2014a; Li et al., 2014b). Identification of affected subpopulations of neurons as well as their synaptic connectivity in future studies will shed some light on the detail mechanism of orofacial neuropathic pain processing post trigeminal nerve injury.

Acknowledgments

Grant information: This study was supported by grants from the National Institutes of Health (DE021847, OS and ZDL; NS064341, ZDL). JP was a recipient of a Pre-Doctoral Fellowship in Pharmacology/Toxicology from the Pharmaceutical Research and Manufacturers of America Foundation (PRMAF-52427).

We would like to thank for the Statistic consulting service provided by The Biostatistics, Epidemiology, and Research Design unit of Institute for Clinical and Translational Science at the University of California, Irvine.

Literature cited

Alvarez FJ, Priestley JV. Anatomy of somatostatin-immunoreactive fibres and cell bodies in the rat trigeminal subnucleus caudalis. Neuroscience. 1990; 38:343–357. [PubMed: 1979854]

Anderson LC, Rao RD. Interleukin-6 and nerve growth factor levels in peripheral nerve and brainstem after trigeminal nerve injury in the rat. Arch Oral Biol. 2001; 46:633–640. [PubMed: 11369318]

Avendano C, Machin R, Bermejo PE, Lagares A. Neuron numbers in the sensory trigeminal nuclei of the rat: A GABA- and glycine-immunocytochemical and stereological analysis. J Comp Neurol. 2005; 493:538–553. [PubMed: 16304625]

Bae YC, Ihn HJ, Park MJ, Ottersen OP, Moritani M, Yoshida A, Shigenaga Y. Identification of signal substances in synapses made between primary afferents and their associated axon terminals in the rat trigeminal sensory nuclei. J Comp Neurol. 2000; 418:299–309. [PubMed: 10701828]

Bae YC, Park KS, Bae JY, Paik SK, Ahn DK, Moritani M, Yoshida A, Shigenaga Y. GABA and glycine in synaptic microcircuits associated with physiologically characterized primary afferents of cat trigeminal principal nucleus. Exp Brain Res. 2005; 162:449–457. [PubMed: 15678357]

Bailey AL, Ribeiro-da-Silva A. Transient loss of terminals from non-peptidergic nociceptive fibers in the substantia gelatinosa of spinal cord following chronic constriction injury of the sciatic nerve. Neuroscience. 2006; 138:675–690. [PubMed: 16413131]

Benes FM, Lange N. Two-dimensional versus three-dimensional cell counting: a practical perspective. Trends in neurosciences. 2001; 24:11–17. [PubMed: 11163882]

Bennetto L, Patel NK, Fuller G. Trigeminal neuralgia and its management. BMJ. 2007; 334:201–205. [PubMed: 17255614]

Braz J, Solorzano C, Wang X, Basbaum AI. Transmitting pain and itch messages: a contemporary view of the spinal cord circuits that generate gate control. Neuron. 2014; 82:522–536. [PubMed: 24811377]

Castro-Lopes JM, Tavares I, Coimbra A. GABA decreases in the spinal cord dorsal horn after peripheral neurectomy. Brain Res. 1993; 620:287–291. [PubMed: 8369960]

Chaplan SR, Bach FW, Pogrel JW, Chung JM, Yaksh TL. Quantitative assessment of tactile allodynia in the rat paw. Journal of neuroscience methods. 1994; 53:55–63. [PubMed: 7990513]

Chery N, Yu XH, de Koninck Y. Visualization of lamina I of the dorsal horn in live adult rat spinal cord slices. J Neurosci Methods. 2000; 96:133–142. [PubMed: 10720677]

Chiang CY, Zhang S, Xie YF, Hu JW, Dostrovsky JO, Salter MW, Sessle BJ. Endogenous ATP involvement in mustard-oil-induced central sensitization in trigeminal subnucleus caudalis (medullary dorsal horn). J Neurophysiol. 2005; 94:1751–1760. [PubMed: 15901761]

Chou AK, Muhammad R, Huang SM, Chen JT, Wu CL, Lin CR, Lee TH, Lin SH, Lu CY, Yang LC. Altered synaptophysin expression in the rat spinal cord after chronic constriction injury of sciatic nerve. Neurosci Lett. 2002; 333:155–158. [PubMed: 12429371]

Darian-Smith C, Hopkins S, Ralston HJ 3rd. Changes in synaptic populations in the spinal dorsal horn following a dorsal rhizotomy in the monkey. J Comp Neurol. 2010; 518:103–117. [PubMed: 19882723]

DeFelipe J, Marco P, Busturia I, Merchan-Perez A. Estimation of the number of synapses in the cerebral cortex: methodological considerations. Cereb Cortex. 1999; 9:722–732. [PubMed: 10554995]

Desmond NL, Levy WB. Changes in the postsynaptic density with long-term potentiation in the dentate gyrus. J Comp Neurol. 1986; 253:476–482. [PubMed: 3025273]

Dixon WJ. Efficient analysis of experimental observations. Annual review of pharmacology and toxicology. 1980; 20:441–462.

Eaton MJ, Plunkett JA, Karmally S, Martinez MA, Montanez K. Changes in GAD- and GABA-immunoreactivity in the spinal dorsal horn after peripheral nerve injury and promotion of recovery by lumbar transplant of immortalized serotonergic precursors. J Chem Neuroanat. 1998; 16:57–72. [PubMed: 9924973]

Eroglu C, Allen NJ, Susman MW, O'Rourke NA, Park CY, Ozkan E, Chakraborty C, Mulinyawe SB, Annis DS, Huberman AD, Green EM, Lawler J, Dolmetsch R, Garcia KC, Smith SJ, Luo ZD, Rosenthal A, Mosher DF, Barres BA. Gabapentin receptor alpha2delta-1 is a neuronal thrombospondin receptor responsible for excitatory CNS synaptogenesis. Cell. 2009; 139:380–392. [PubMed: 19818485]

Gobel S. Golgi studies of the neurons in layer II of the dorsal horn of the medulla (trigeminal nucleus caudalis). J Comp Neurol. 1978; 180:395–413. [PubMed: 659668]

Hockfield S, Gobel S. An anatomical demonstration of projections to the medullary dorsal horn (trigeminal nucleus caudalis) from rostral trigeminal nuclei and the contralateral caudal medulla. Brain Res. 1982; 252:203–211. [PubMed: 6185175]

Hu JW. Response properties of nociceptive and non-nociceptive neurons in the rat's trigeminal subnucleus caudalis (medullary dorsal horn) related to cutaneous and deep craniofacial afferent stimulation and modulation by diffuse noxious inhibitory controls. Pain. 1990; 41:331–345. [PubMed: 2388770]

Huang D, Yu B. The mirror-image pain: an unclered phenomenon and its possible mechanism. Neuroscience and biobehavioral reviews. 2010; 34:528–532. [PubMed: 19883682]

Ibuki T, Hama AT, Wang XT, Pappas GD, Sagen J. Loss of GABA-immunoreactivity in the spinal dorsal horn of rats with peripheral nerve injury and promotion of recovery by adrenal medullary grafts. Neuroscience. 1997; 76:845–858. [PubMed: 9135056]

Iwata K, Imai T, Tsuboi Y, Tashiro A, Ogawa A, Morimoto T, Masuda Y, Tachibana Y, Hu J. Alteration of medullary dorsal horn neuronal activity following inferior alveolar nerve transection in rats. J Neurophysiol. 2001; 86:2868–2877. [PubMed: 11731543]

Iwata K, Imamura Y, Honda K, Shinoda M. Physiological mechanisms of neuropathic pain: the orofacial region. Int Rev Neurobiol. 2011; 97:227–250. [PubMed: 21708313]

Iwata K, Masuda Y, Ren K. Trigeminal neuronal recording in animal models of orofacial pain. Methods Mol Med. 2004; 99:123–137. [PubMed: 15131334]

Jacquin MF, Chiaia NL, Rhoades RW. Trigeminal projections to contralateral dorsal horn: central extent, peripheral origins, and plasticity. Somatosens Mot Res. 1990; 7:153–183. [PubMed: 2378191]

Jacquin MF, Golden J, Rhoades RW. Structure-function relationships in rat brainstem subnucleus interpolaris: III. Local circuit neurons. J Comp Neurol. 1989; 282:24–44. [PubMed: 2708592]

Julius D, Basbaum AI. Molecular mechanisms of nociception. Nature. 2001; 413:203–210. [PubMed: 11557989]

Kato G, Kawasaki Y, Koga K, Uta D, Kosugi M, Yasaka T, Yoshimura M, Ji RR, Strassman AM. Organization of intralaminar and translaminar neuronal connectivity in the superficial spinal dorsal horn. J Neurosci. 2009; 29:5088–5099. [PubMed: 19386904]

Kernisant M, Gear RW, Jasmin L, Vit JP, Ohara PT. Chronic constriction injury of the infraorbital nerve in the rat using modified syringe needle. J Neurosci Methods. 2008; 172:43–47. [PubMed: 18501433]

Kim DS, Li KW, Boroujerdi A, Peter Yu Y, Zhou CY, Deng P, Park J, Zhang X, Lee J, Corpe M, Sharp K, Steward O, Eroglu C, Barres B, Zaucke F, Xu ZC, Luo ZD. Thrombospondin-4 contributes to spinal sensitization and neuropathic pain states. J Neurosci. 2012; 32:8977–8987. [PubMed: 22745497]

Labrakakis C, Lorenzo LE, Bories C, Ribeiro-da-Silva A, De Koninck Y. Inhibitory coupling between inhibitory interneurons in the spinal cord dorsal horn. Mol Pain. 2009; 5:24. [PubMed: 19432997]

Leo S, Moechars D, Callaerts-Vegh Z, D'Hooge R, Meert T. Impairment of VGLUT2 but not VGLUT1 signaling reduces neuropathy-induced hypersensitivity. Eur J Pain. 2009; 13:1008–1017. [PubMed: 19171494]

Li KW, Kim DS, Zaucke F, Luo ZD. Trigeminal nerve injury-induced thrombospondin-4 up-regulation contributes to orofacial neuropathic pain states in a rat model. Eur J Pain. 2014a; 18:489–495. [PubMed: 24019258]

Li KW, Yu YP, Zhou C, Kim DS, Lin B, Sharp K, Steward O, Luo ZD. Calcium channel alpha2delta1 proteins mediate trigeminal neuropathic pain states associated with aberrant excitatory synaptogenesis. J Biol Chem. 2014b; 289:7025–7037. [PubMed: 24459143]

Lo FS, Zhao S, Erzurumlu RS. Astrocytes promote peripheral nerve injury-induced reactive synaptogenesis in the neonatal CNS. J Neurophysiol. 2011; 106:2876–2887. [PubMed: 21900512]

Lu Y, Dong H, Gao Y, Gong Y, Ren Y, Gu N, Zhou S, Xia N, Sun YY, Ji RR, Xiong L. A feed-forward spinal cord glycinergic neural circuit gates mechanical allodynia. J Clin Invest. 2013; 123:4050–4062. [PubMed: 23979158]

Lu Y, Perl ER. Modular organization of excitatory circuits between neurons of the spinal superficial dorsal horn (laminae I and II). J Neurosci. 2005; 25:3900–3907. [PubMed: 15829642]

Martin YB, Malmierca E, Avendano C, Nunez A. Neuronal disinhibition in the trigeminal nucleus caudalis in a model of chronic neuropathic pain. Eur J Neurosci. 2010; 32:399–408. [PubMed: 20704591]

Maxwell DJ, Belle MD, Cheunsuang O, Stewart A, Morris R. Morphology of inhibitory and excitatory interneurons in superficial laminae of the rat dorsal horn. The Journal of physiology. 2007; 584:521–533. [PubMed: 17717012]

Milligan ED, Twining C, Chacur M, Biedenkapp J, O'Connor K, Poole S, Tracey K, Martin D, Maier SF, Watkins LR. Spinal glia and proinflammatory cytokines mediate mirror-image neuropathic pain in rats. J Neurosci. 2003; 23:1026–1040. [PubMed: 12574433]

Miraucourt LS, Dallel R, Voisin DL. Glycine inhibitory dysfunction turns touch into pain through PKCgamma interneurons. PLoS One. 2007; 2:e1116. [PubMed: 17987109]

Miraucourt LS, Moisset X, Dallel R, Voisin DL. Glycine inhibitory dysfunction induces a selectively dynamic, morphine-resistant, and neurokinin 1 receptor- independent mechanical allodynia. J Neurosci. 2009; 29:2519–2527. [PubMed: 19244526]

Moore KA, Kohno T, Karchewski LA, Scholz J, Baba H, Woolf CJ. Partial peripheral nerve injury promotes a selective loss of GABAergic inhibition in the superficial dorsal horn of the spinal cord. J Neurosci. 2002; 22:6724–6731. [PubMed: 12151551]

Morris R, Cheunsuang O, Stewart A, Maxwell D. Spinal dorsal horn neurone targets for nociceptive primary afferents: do single neurone morphological characteristics suggest how nociceptive information is processed at the spinal level. Brain Res Brain Res Rev. 2004; 46:173–190. [PubMed: 15464206]

Oliveira AL, Hydling F, Olsson E, Shi T, Edwards RH, Fujiyama F, Kaneko T, Hokfelt T, Cullheim S, Meister B. Cellular localization of three vesicular glutamate transporter mRNAs and proteins in rat spinal cord and dorsal root ganglia. Synapse. 2003; 50:117–129. [PubMed: 12923814]

Panneton WM, Klein BG, Jacquin MF. Trigeminal projections to contralateral dorsal horn originate in midline hairy skin. Somatosens Mot Res. 1991; 8:165–173. [PubMed: 1887727]

Pierce JP, Lewin GR. An ultrastructural size principle. Neuroscience. 1994; 58:441–446. [PubMed: 8170532]

Polgar E, Gray S, Riddell JS, Todd AJ. Lack of evidence for significant neuronal loss in laminae I-III of the spinal dorsal horn of the rat in the chronic constriction injury model. Pain. 2004; 111:144–150. [PubMed: 15327818]

Polgar E, Hughes DI, Riddell JS, Maxwell DJ, Puskar Z, Todd AJ. Selective loss of spinal GABAergic or glycinergic neurons is not necessary for development of thermal hyperalgesia in the chronic constriction injury model of neuropathic pain. Pain. 2003; 104:229–239. [PubMed: 12855333]

Ribeiro-da-Silva A, Tagari P, Cuello AC. Morphological characterization of substance P-like immunoreactive glomeruli in the superficial dorsal horn of the rat spinal cord and trigeminal subnucleus caudalis: a quantitative study. J Comp Neurol. 1989; 281:497–415. [PubMed: 2468697]

Rogoz K, Lagerstrom MC, Dufour S, Kullander K. VGLUT2-dependent glutamatergic transmission in primary afferents is required for intact nociception in both acute and persistent pain modalities. Pain. 2012; 153:1525–1536. [PubMed: 22633683]

Sandkuhler J. Models and mechanisms of hyperalgesia and allodynia. Physiol Rev. 2009; 89:707–758. [PubMed: 19342617]

Santos SF, Luz LL, Szucs P, Lima D, Derkach VA, Safronov BV. Transmission efficacy and plasticity in glutamatergic synapses formed by excitatory interneurons of the substantia gelatinosa in the rat spinal cord. PLoS ONE. 2009; 4:e8047. [PubMed: 19956641]

Sessle BJ. Acute and chronic craniofacial pain: brainstem mechanisms of nociceptive transmission and neuroplasticity, and their clinical correlates. Crit Rev Oral Biol Med. 2000; 11:57–91. [PubMed: 10682901]

Somers DL, Clemente FR. Dorsal horn synaptosomal content of aspartate, glutamate, glycine and GABA are differentially altered following chronic constriction injury to the rat sciatic nerve. Neurosci Lett. 2002; 323:171–174. [PubMed: 11959412]

Takazawa T, MacDermott AB. Glycinergic and GABAergic tonic inhibition fine tune inhibitory control in regionally distinct subpopulations of dorsal horn neurons. The Journal of physiology. 2010; 588:2571–2587. [PubMed: 20498232]

Todd AJ. GABA and glycine in synaptic glomeruli of the rat spinal dorsal horn. Eur J Neurosci. 1996; 8:2492–2498. [PubMed: 8996798]

Todd AJ. Neuronal circuitry for pain processing in the dorsal horn. Nat Rev Neurosci. 2010; 11:823–836. [PubMed: 21068766]

Todd AJ, Hughes DI, Polgar E, Nagy GG, Mackie M, Ottersen OP, Maxwell DJ. The expression of vesicular glutamate transporters VGLUT1 and VGLUT2 in neurochemically defined axonal populations in the rat spinal cord with emphasis on the dorsal horn. Eur J Neurosci. 2003; 17:13–27. [PubMed: 12534965]

Todd AJ, Spike RC, Polgar E. A quantitative study of neurons which express neurokinin-1 or somatostatin sst2a receptor in rat spinal dorsal horn. Neuroscience. 1998; 85:459–473. [PubMed: 9622244]

Tsuboi Y, Takeda M, Tanimoto T, Ikeda M, Matsumoto S, Kitagawa J, Teramoto K, Simizu K, Yamazaki Y, Shima A, Ren K, Iwata K. Alteration of the second branch of the trigeminal nerve activity following inferior alveolar nerve transection in rats. Pain. 2004; 111:323–334. [PubMed: 15363876]

Vos BP, Strassman AM, Maciewicz RJ. Behavioral evidence of trigeminal neuropathic pain following chronic constriction injury to the rat's infraorbital nerve. J Neurosci. 1994; 14:2708–2723. [PubMed: 8182437]

Yasaka T, Kato G, Furue H, Rashid MH, Sonohata M, Tamae A, Murata Y, Masuko S, Yoshimura M. Cell-type-specific excitatory and inhibitory circuits involving primary afferents in the substantia gelatinosa of the rat spinal dorsal horn in vitro. J Physiol. 2007; 581:603–618. [PubMed: 17347278]

Yasaka T, Tiong SY, Hughes DI, Riddell JS, Todd AJ. Populations of inhibitory and excitatory interneurons in lamina II of the adult rat spinal dorsal horn revealed by a combined electrophysiological and anatomical approach. Pain. 2010; 151:475–488. [PubMed: 20817353]

Zakrzewska JM, McMillan R. Trigeminal neuralgia: the diagnosis and management of this excruciating and poorly understood facial pain. Postgraduate medical journal. 2011; 87:410–416. [PubMed: 21493636]

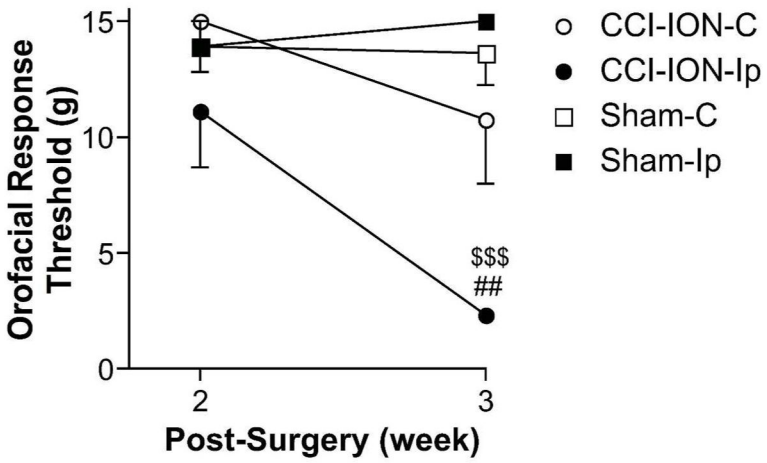

Figure 1.

Unilateral chronic constriction injury to the infraorbital nerve (CCI-ION) caused orofacial hypersensitivity to mechanical stimuli at three-weeks post-surgery in rats. Sensitivity to von Frey filament stimulation on the whisker pad was tested two- and three-weeks post CCI-ION or sham operations. Data presented are the means ± SEM from 3 rats for each group. Ip, ipsilateral to injury; C, contralateral to injury. $^{\#\#}p < 0.01$ compared to CCI-ION-C; $^{\$\$\$}p < 0.001$ compared to sham-Ip by Two-Way ANOVA with Bonferroni post hoc test.

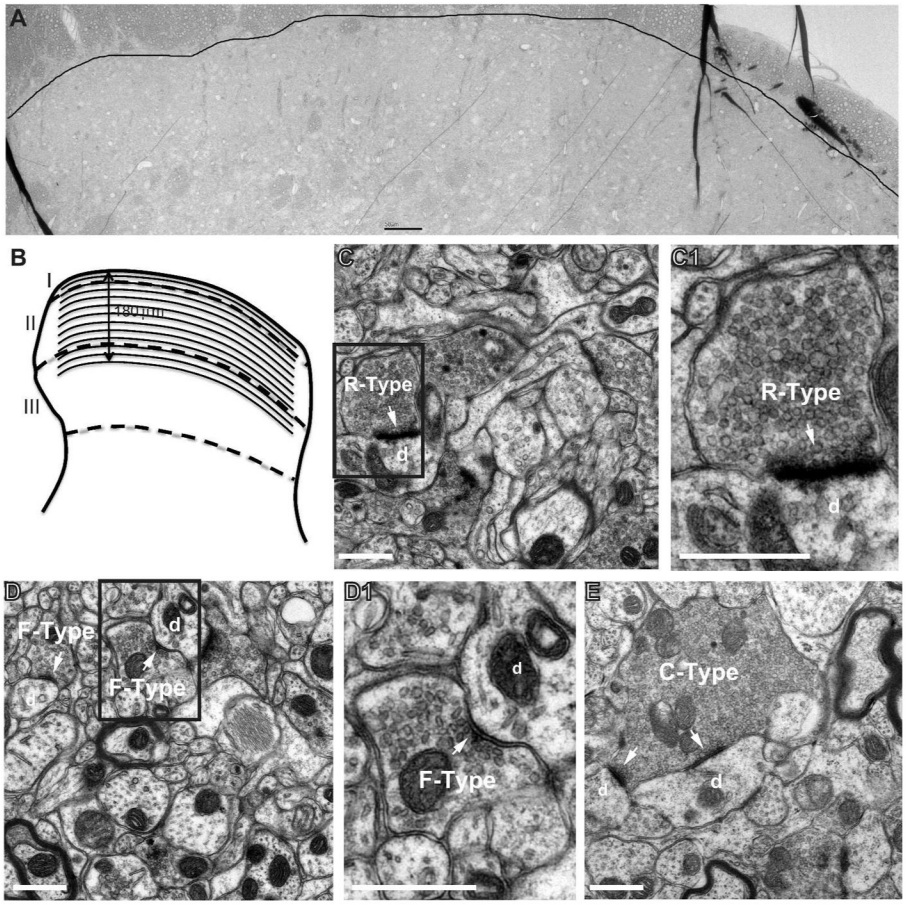

Figure 2.

Sampling method and different synaptic profiles in electron micrographs of Vc/C2 superficial dorsal horn from CCI-ION rats. **A.** Three merged electron micrographs showing the entire sample region of the superficial dorsal horn of CCI-ION rats. Scale bar = 50μm. **B.** Schematic diagram of the dorsal horn grey matter with the sampling area covered by 12 parallel sampling tracks orthogonal to the curve of the dorsal horn, and crossing the predicted superficial laminae (dorso-ventral) outlined by dotted lines. **C,** a representative R-type terminal (arrow) with a large synaptic profile and uniform round vesicles typical of an excitatory synapse; **C1**, enlarged rectangle region in **C. D,** Representative F-type terminals (arrows) with pleomorphic vesicles and synapse typical of an inhibitory synapse; **D1,** enlarged rectangle region in **D. E.** A representative C-type primary afferent terminal synapsing with multiple dendrites (arrows). d. dendrite. Scale bars = 0.5μm for C–E.

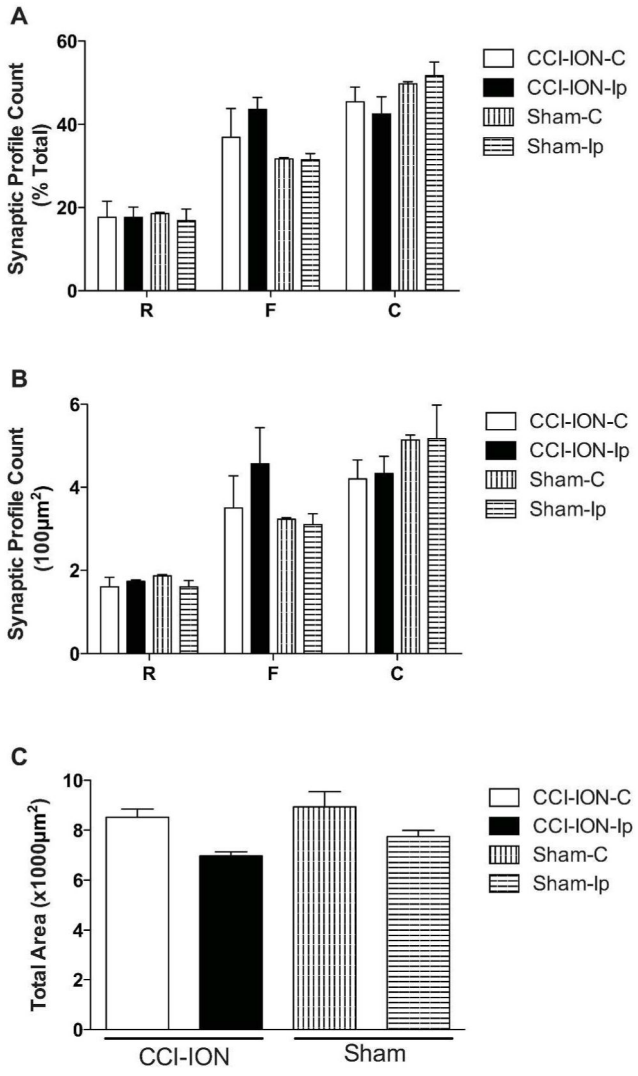

Figure 3.

Quantification of total synaptic profile counts in Vc/C2 dorsal horn of CCI-ION and sham rats. **A, B:** Summarized data of the proportion of each synaptic profile (R, F, and C) per total profile count (**A**) or per 100μm^2 (**B**) through superficial dorsal horn. **C:** Summarized data of the total area of tissue examined. Data presented are the means ± SEM from 3 rats for each group. Ip, ipsilateral to injury; C, contralateral to injury.

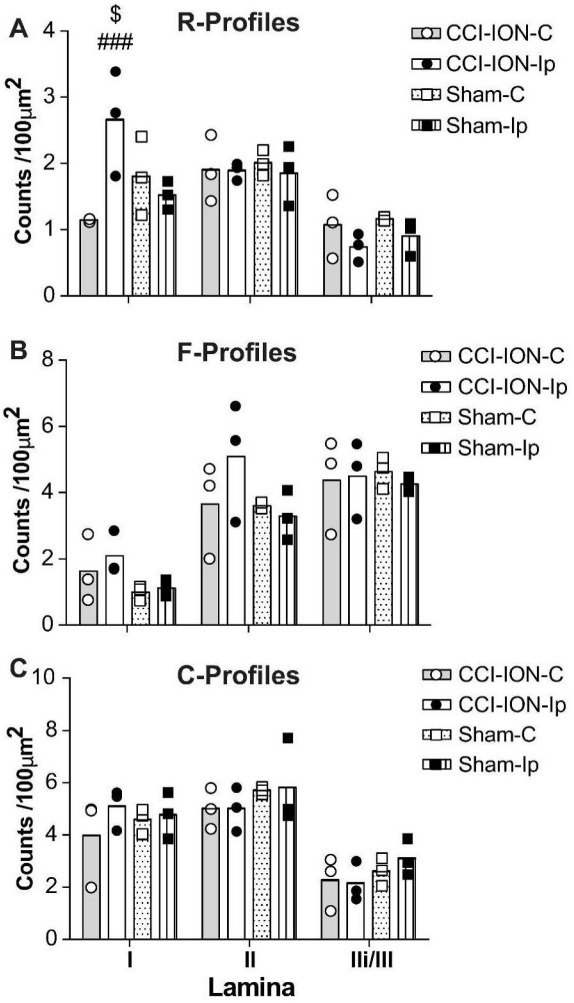

Figure 4.

Bar graph of overall mean values of R- (**A**), F- (**B**), and C- (**C**) profile counts per 100μm^2 through superficial dorsal horn of Vc/C2 in each group with the distribution of individual means from each rat indicated. Data from tracks within the predicted thickness of lamina I (0–30μm), lamina II (30–135μm), and lamina IIi/III (135–180μm) were combined. $^{###}p < 0.001$ (p=0.0009) compared with CCI-ION-C; $^{\$}p < 0.05$ (p=0.0167) compared with sham-Ip by Two-Way ANOVA with Bonferroni post hoc test. Ip, ipsilateral to injury; C, contralateral to injury.

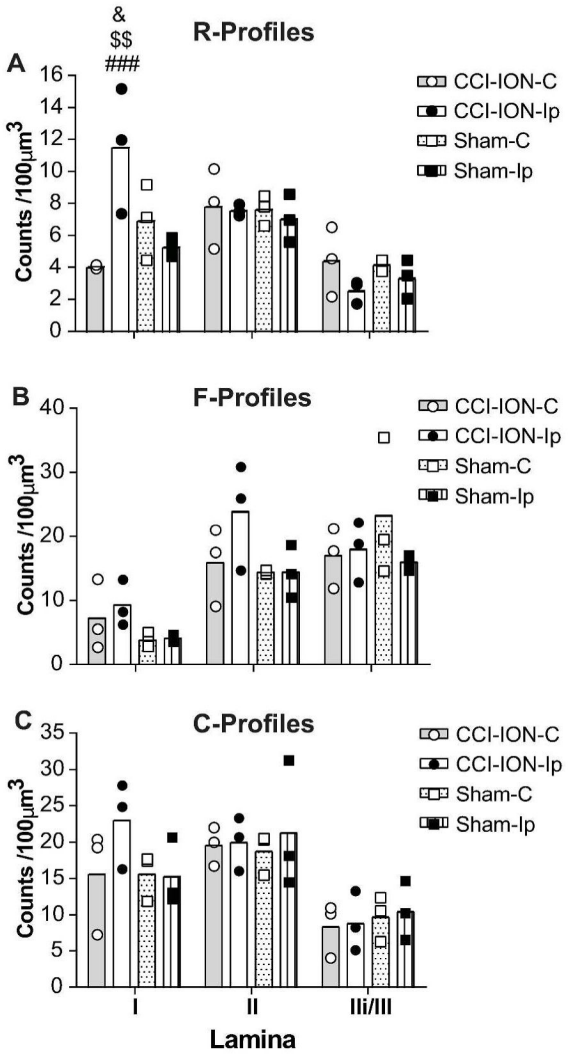

Figure 5.

Bar graph of overall mean values of R- (**A**), F- (**B**), and C- (**C**) profile counts using the size-frequency method (profile/100μm^3) through superficial dorsal horn of Vc/C2 with the distribution of individual means from each rat indicated. Data from tracks within the predicted thickness of lamina I (0–30μm), lamina II (30–135μm), and lamina IIi/III (135–180μm) were combined. $^{###}p < 0.001$ (p=0.0003) compared with CCI-ION-C; $^{\$\$}p < 0.01$ (p=0.0023) compared with sham-Ip, and $^{\&}p < 0.05$ (p=0.038) compared with sham-C by Two-Way ANOVA with Bonferroni post hoc test. Ip, ipsilateral to injury; C, contralateral to injury.

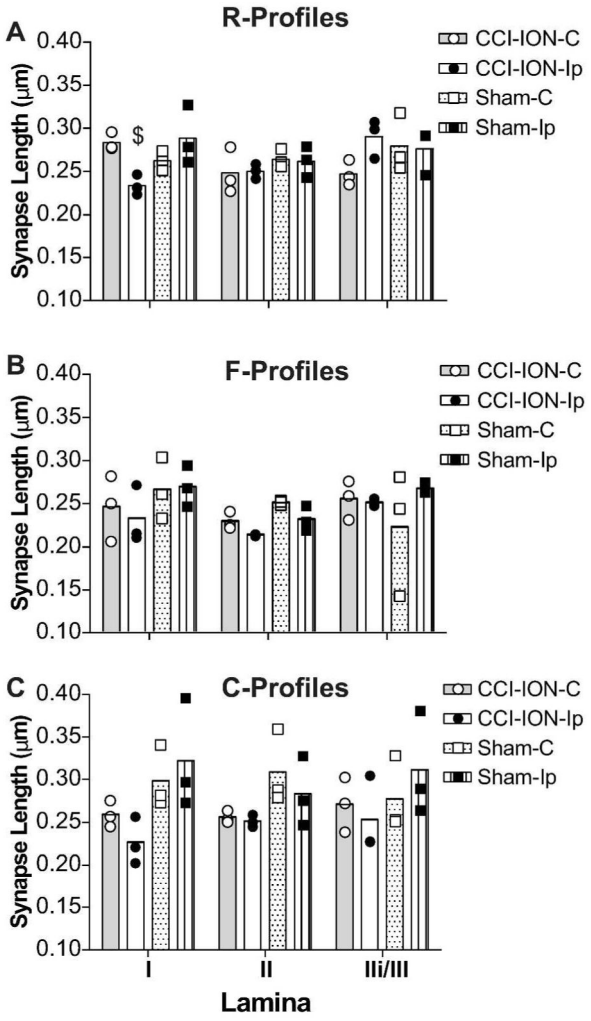

Figure 6.

Bar graph of overall mean values of synaptic length for R- (**A**), F- (**B**), and C- (**C**) profiles through superficial dorsal horn of Vc/C2 with the distribution of individual means from each rat indicated. Data from tracks within the predicted thickness of lamina I (0–30μm), lamina II (30–135μm), and lamina IIi/III (135–180μm) were combined. $^{\$}p < 0.05$ (p=0.0349) compared with sham-Ip by Two-Way ANOVA with Bonferroni post hoc test. Ip, ipsilateral to injury; C, contralateral to injury.

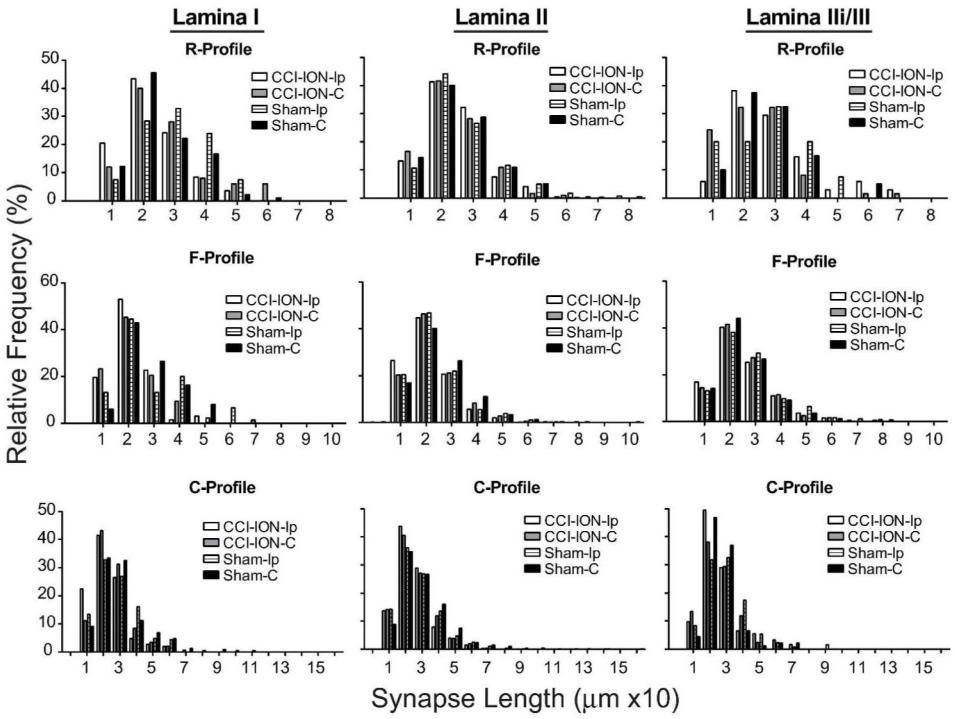

Figure 7.

Relative frequency histogram of synaptic lengths for R-, F-, and C-Profiles through the superficial dorsal horn of Vc/C2. Data are in bins of 0.1µm and measured within the predicted thickness of lamina I (0–30µm), lamina II (30–135µm), and lamina IIi/III (135–180µm) for each experimental group.

Table 1

Profile counts within Vc/C2 dorsal horn of 3-week CCI-ION or Sham rats

Contralateral Side (non-injured side)											
			R-Profiles			F-Profiles			C-Profiles		
Animal ID	**Total Counts**	**Total Area (μm²)**	**Counts**	**Counts/ Total Counts (%)**	**Counts/ 100μm²**	**Counts**	**Counts/ Total Counts (%)**	**Counts/ 100μm²**	**Counts**	**Counts/ Total Counts (%)**	**Counts/ 100μm²**
CCI-ION											
1	813	8600	103	12.7	1.2	398	49.0	4.6	312	38.4	3.6
2	841	7938	126	15	1.6	308	36.6	3.9	407	48.4	5.1
3	711	9049	180	25.3	2.0	179	25.2	2.0	352	49.5	3.9
Sham											
1	904	8652	167	18.5	1.9	281	31.1	3.2	456	50.4	5.3
2	803	8070	153	19.1	1.9	258	32.1	3.2	392	48.8	4.9
3	1041	10108	186	17.9	1.8	333	32.0	3.3	522	50.1	5.2

Ipsilateral Side (injured side)											
			R-Profiles			F-Profiles			C-Profiles		
Animal ID	**Total Counts**	**Total Area (μm²)**	**Counts**	**Counts/ Total Counts (%)**	**Counts/ 100μm²**	**Counts**	**Counts/ Total Counts (%)**	**Counts/ 100μm²**	**Counts**	**Counts/ Total Counts (%)**	**Counts/ 100μm²**
CCI-ION											
1	779	6615	122	15.7	1.8	382	49.0	5.8	275	35.3	4.2
2	846	7144	123	14.5	1.7	360	42.6	5.0	363	42.9	5.1
3	526	7118	119	22.6	1.7	206	39.2	2.9	260	49.4	3.7
Sham											
1	752	8229	138	18.4	1.7	260	34.6	3.2	354	47.1	4.3
2	656	7382	136	20.7	1.8	192	29.3	2.6	328	50.0	4.4
3	885	7594	102	11.5	1.3	269	30.4	3.5	514	58.1	6.8

Total numbers of synaptic profile counts for 12 tracks in superficial dorsal horn of Vc/C2 from each animal. Profile counts are expressed per 100μm^2 or as proportion of synaptic profile counts over total profile counts.

Table 2

Univariate analyses of variance for different synaptic profile types

	Counts/100μm^2			Counts/100μm^3			Synapse Length		
Synaptic Type	**R**	**F**	**C**	**R**	**F**	**C**	**R**	**F**	**C**
Group Interactions	F=3.017	F=1.847	F=0.518	F=4.118	F=1.975	F=1.041	F=4.613	F=1.009	F=2.061
	p=0.036	p=0.153	p=0.786	p=0.010	p=0.130	p=0.436	p=0.007	p=0.453	p=0.116
Injury-induced Effect	F=2.463	F=0.785	F=0.778	F=2.549	F=0.950	F=0.363	F=0.751	F=1.074	F=1.923
	p=0.137	p=0.535	p=0.538	p=0.130	p=0.461	p=0.781	p=0.552	p=0.413	p=0.204
Lamina specificity	F=18.20	F=104.1	F=37.43	F=16.11	F=33.18	F=22.52	F=3.398	F=1.803	F=0.075
	p=0.000	p=0.000	p=0.000	p=0.000	p=0.000	p=0.000	p=0.059	p=0.197	p= 0.927

Statistical analyses of four experimental group (CCI-ION-Ip, CCI-ION-C, sham-Ip, and sham-C) and lamina interactions using a mixed Two-Way ANOVA analysis.

Gray area highlight statistically significant changes